PHYSA 8216
pp: 1--7 (col.fig.: Nil)
PROD. TYPE: COM
ED: Preetha
PAGN: Suresh – SCAN: Padma
ARTICLE IN PRESS
Available online at www.sciencedirect.com
SCIENCE DIRECT®
PHYSICA A
ELSEVIER
Physica A ▮▮▮ (▮▮▮▮) ▮▮▮–▮▮▮
www.elsevier.com/locate/physa

A rhombohedral family of minimal surfaces as a pathway between the P and D cubic mesophases

G.E. Schröder[a,*], S.J. Ramsden[a,b], A. Fogden[c], S.T. Hyde[a]

[a] *Department of Applied Mathematics, RSPhysSE, Australian National University, Canberra 0200 ACT, Australia*

[b] *Supercomputer Facility, Australian National University, Canberra 0200 ACT, Australia*

[c] *Institute for Surface Chemistry, P.O. Box 5607, Stockholm SE-11486, Sweden*

Abstract

A medial surface (MS) analysis of the rhombohedral infinite periodic minimal surface family rPD is presented. The rPD family of bicontinuous surfaces has been suggested as a pathway for transitions between its two cubic members, the P and the D surface, in mesophases in liquid-crystalline self-assembly. The MS is a representation of a labyrinth as a centered 2D skeleton. By providing a definition of a pointwise channel diameter, the MS allows for an analysis of stretching frustration and homogeneity of such surfaces. For the rPD surface, variations of this channel diameter are locally minimal for the D surface, and a horizontal inflection point for the P surface. This may have implications for the phase stability of the corresponding liquid-crystalline mesophases. The MS can be further reduced to a 1D line graph. This graph contains curved edges and cannot be deduced from symmetry considerations alone.

PACS: 02.40. – k; 81.16.Dn; 61.30.St; 02.70. – c

Keywords: Periodic minimal surfaces; Self-assembly; Lyotropic phases

Bicontinuous infinite periodic minimal surfaces (IPMS) are surfaces that divide space into two intertwined labyrinths, and that are minimal surfaces everywhere. Among the best-known examples are (1) the P(rimitive) surface that is the balanced interface between two interlocked simple cubic lattices that have the same orientation, but are offset by half a body diagonal, and (2) the D(iamond) surface that is the balanced interface between two intertwined Diamond lattices. Both are of cubic symmetry.

* Corresponding author.
E-mail address: gerd.schroeder@anu.edu.au (G.E. Schröder).

0378-4371/$ - see front matter
doi:10.1016/j.physa.2004.03.056

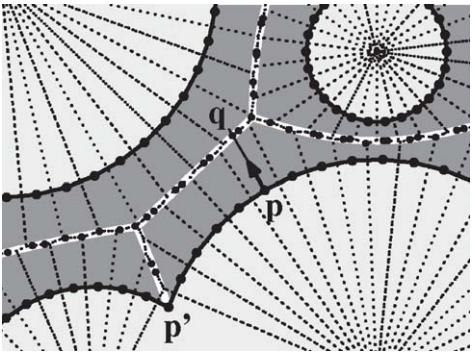

Fig. 1. Illustration of the medial axis for a planar situation: The domain C (dark gray) is the complement of an assembly of overlapping disks (light gray). The boundary ∂C of the domain is discretized into vertices V (black points) connected by edges. The interface normal vectors are pointing into C. The first step is the computation of the Voronoi diagram of the set of vertices V (dashed lines). For every point $p \in \partial C$ there is a corresponding point q on the MS which is the intersection of the straight line in normal direction through p with the Voronoi cell of p. The white line is the exact medial axis for which an analytic form is known in the case of disk assemblies [8].

Bicontinuous morphologies based on IPMS describe well the spatial structure of many condensed molecular systems, including lyotropic liquid crystals [1,2], zeolites [2], synthetic surfactant systems [3] and biological membranes [4] including the lung alveolar surface [5]. All examples known to date, except the last one, adopt cubic symmetries.

Although most bicontinuous structures reported in the literature are of cubic symmetry there are compelling reasons to study non-cubic IPMS. First, they might serve as possible dynamic transition structures between stable cubic phases, has been suggested in recent experimental work [6]. Second, the prevalence of cubic IPMS in physical systems demands exploration. That issue is best addressed by studying surface families that are in general not cubic, but comprise singular members with cubic symmetry, such as the rPD.

The link between surface geometry and physics can be made using surface energy functionals. The relevant functional for self-assembly of amphiphiles is often based on the so-called Helfrich free-energy functional that gives the intrinsic free energy in terms of the interfacial curvature characteristics [7]. This reduces amphiphile assemblies to fictional surfaces of zero thickness. Yet, in many cases non-local interactions and channel diameter variations (due to chain stretching contributions of individual amphiphile molecules) need to be taken into account. Our analysis shows one route to including these global effects in measures of relative stability of various morphologies (Fig. 1).

1. Definition and computation of the medial surface

The medial surface transform is a complete description of a surface in terms of a geometrically centered skeleton [9]: any object (here one of the two channels of an

IPMS) is represented by a, in some sense minimal, union of balls centered on a 2D skeleton that is symmetrically located inside the object.

Here we define and summarize the main properties of the MS construction and describe an algorithm for MS computations of triangulated surfaces derived from mathematical models. A more detailed discussion can be found in our previous article [10].

We define a domain C to be an open, connected subset of 3d euclidean space ($\mathbb{E}^3$) whose boundary, $S = \partial C$, is an oriented and $\mathscr{C}^2$-smooth manifold. In this article, C is one of the two subvolumes bounded by an IPMS and S is the IPMS itself. A smooth normal field N is defined on S, and we assume the normals to be of unit length and pointing into the domain C.

The MS is the set of points in C with two or more nearest points on the domain boundary S. Equivalently, it is the locus of centers of maximal spheres in C, i.e., those spheres contained in C which are not contained in any other sphere in C and, consequently, graze S [9].

Loosely speaking, the MS defines the center of the domain C. For the case of surfaces bounding a labyrinth—as for the IPMS discussed here—the MS is a two-dimensional skeleton that is geometrically centered within the channels. In general, the MS consists of a collection of surface patches meeting along one-dimensional curves. In particular cases, the patches may extend to infinity, or degenerate to one-dimensional curves or even points.

For any point $p \in S$ on the boundary S of the domain C there is exactly one corresponding point $q := ms(p)$ on the MS of C; the converse is not true. The point p is located at the shortest distance from q compared with all other points on S. The map ms from a point $p \in S$ to the corresponding MS point $q = ms(p)$ can be written as

$$ms : S \to \mathbb{E}^3, \quad p \mapsto ms(p) := p + d(p)N(p)\,, \tag{1}$$

where N is the normal field of S and $d : S \to \mathbb{R}^+$ is called the distance (or radius) function.

Analytic computations of the MS are rarely possible, even for domains derived from mathematically parametrized surfaces. For triangulated surface representations, identification of the MS as a subset of the Voronoi diagram of the sample points provides a numerical approach to MS computations. This has been suggested by a number of authors, e.g. in Ref. [11], and an adaption to parametrized surfaces is described in our previous article [10].

Voronoi-based MS algorithms neatly combine two ideas that are loosely summarized as follows: given a point p on S (say part of an imaginary triangulation of S), the first observation is that the corresponding MS point is locally maximally distant from the surface patch containing p. Therefore, the corresponding MS point is meant to lie in normal direction, as stated as well in Eq. (1). Second, since it is equidistant from at least two surface points, it approximately lies on one of the faces of the Voronoi diagram of the vertices V of the triangulation of S. This is because the Voronoi diagram of the set of vertices V gives exactly the locus of points equidistant from two out of the vertices in V.

Therefore, the following algorithm computes an approximation to the MS that converges to the exact MS if the sampling density goes to infinity [11]. Given is a set

of vertices V where each vertex $p \in V$ is a point exactly on S (no out-of-surface noise). (1) Determine the Voronoi diagram of the point set V in $\mathbb{E}^3$. (2) For each point $p \in V$ intersect the straight line in normal direction, $p + rN(p)$ with $r \in \mathbb{R}^+$, with the Voronoi cell of the point p. The triangulation itself can be taken to be the same as on the original surface.

The MS can be further reduced to a line graph. The guiding idea is that this path through the tunnel system is maximally distant from the original surface and retains its topology. As the MS is centered within the channel system, the line graph should lie in the MS. Within the MS the graph is meant to be at maximal distance from the IPMS: therefore we define the graph to be the set of critical paths with respect to $d(p)$ on the surface that connect critical points of d to each other—much in the spirit of determining ridge lines in a 2D topography. These paths can either be determined on the MS, or on the IPMS and then mapped onto MS. Here we present data using the latter approach. This graph contains some edges that need to be discarded based on a topological criterion (for details see Ref. [10]).

2. MS structure of the rPD surface family

The rPD surface family is a one-parameter family of surfaces that remains triply-periodic, bicontinuous, embedded and minimal for all values of the free parameter $r_0 \in [0, \infty]$. For the specific values $r_0 = 1/\sqrt{2}$ and $r_0 = \sqrt{2}$ the rPD corresponds to the P and D surface, respectively. Thus it provides a pathway of continuous and embedded space partitions between these two cubic IPMS, with each intermediate itself an IPMS. [1]

All minimal surfaces in $\mathbb{E}^3$ can be parametrized by a Weierstrass representation, i.e., a parametrization of the surface as path integrals mapping the complex plane into $\mathbb{E}^3$. The numerical calculations presented later are all based on surface data generated from this exact approach; see Refs. [12,13] for details.

Alternatively, the rPD is the minimal surface spanning two parallel, horizontal equilateral triangles a distance c^* apart that are rotated by 60° around the vertical line; by simple rotations in $\mathbb{E}^3$ an IPMS can be generated from that catenoidal surface element; the parameter c^* can be expressed in terms of r_0. The point-wise defined distance function $d(p)$, see Eq. (1), defines a channel diameter that varies over the surface. As introduced in Ref. [10] the fluctuations of that distance over the surface provide a measure for homogeneity of the structure. In the case of type II mesophases they can be linked to chain stretching contributions to the free energy (as compared to bending terms) (Fig. 2).

We define a hypothetical perfectly homogeneous surface as one whose curvatures and distance function remain constant at all points on the surface. Such a homogeneous structure cannot be immersed in $\mathbb{E}^3$; for hyperbolic surfaces variations of both the Gaussian curvature and the distance function cannot be avoided. For IPMS a measure

[1] The Bonnet relation between the P and D surfaces suggests another such surface family that is obtained by simply varying the Bonnet angle and that is by definition isometric. That surface family is not embedded, i.e., not free of self-intersections. The rPD is free of self-intersections, but the members are not isometric.

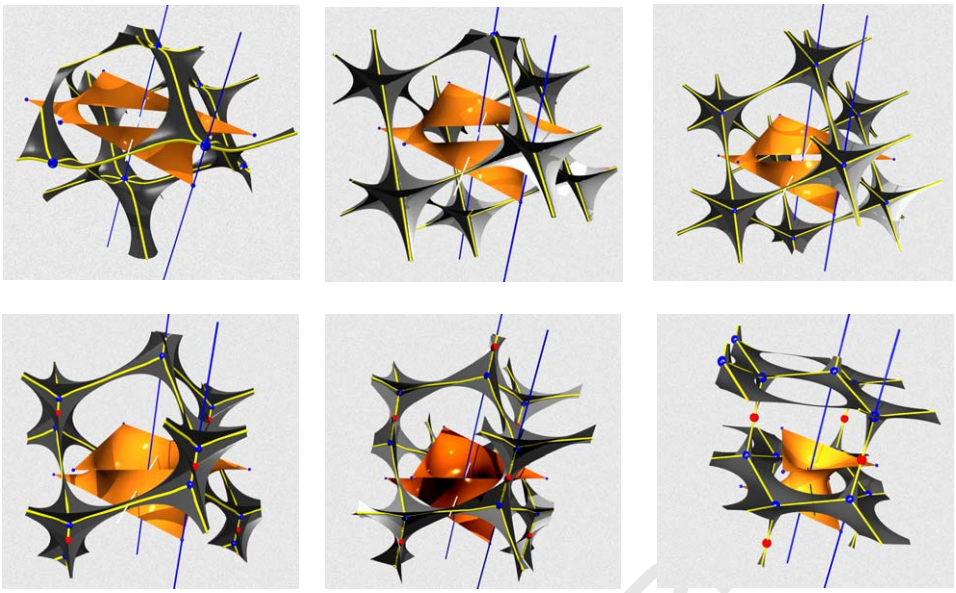

Fig. 2. MS structure of the rPD family for different values of the free parameter r_0. The images show the MS for the following values of r_0 (top left to bottom right): 0.45, 0.65, $1/\sqrt{2}$ (P), 0.85, 1.05, 2.25. The member corresponding to the D surface, $r_0 = \sqrt{2}$, is not shown. Shown are portions of the MS (dark gray) and the line graph (light lines) to which the MS is reduced. Also shown is the characteristic rPD minimal surface piece stretched over two triangles at distance c^* and twisted by 60°, as well as two three-fold axes (vertical straight lines) and a 2-fold axis (horizontal straight line). The first image shows clearly that no graph with only straight edges could be embedded in the MS neighboring pairs of six-connected nodes lie in mirror planes (the foreground clipping plane) and cannot be connected by a straight line contained in the MS. The nodes of the graph are at symmetry sites of the $R\bar{3}m$ space group only for $r_0 < 1/\sqrt{2}$. For $r_0 > 1/\sqrt{2}$ (and $r_0 \neq \sqrt{2}$), they are in general position.

for the chain stretching homogeneity is then given by the fluctuations of $d(p)$ around the mean value $\langle d\rangle = (1/A)\int d(p)\,\mathrm{d}p$ where the integral is over a representative surface patch and A is its area. Here we analyze these fluctuations in terms of their mean square fluctuations $(\Delta d)^2 = \langle (d - \langle d\rangle)^2\rangle$.

Fig. 3 shows the fluctuations Δd as a function of r_0. The length scale of the surface remains a free parameter, allowing for different normalizations. We present the fluctuations scaled by two possible constants: first relative to the mean distance function value $\langle d\rangle$ (relevant if the system exhibits a preferred diameter, as in a dense molecular packing), and second normalized such that the ratio of surface to volume remains constant (relevant to a transition between two lyotropic phases at fixed solvent volume).

The key observation is that the D surface corresponds to a minimum of the fluctuations Δd, whereas the P surface seems to be a horizontal inflection point of Δd. If variations of d are penalized the D surface should be more stable than the P surface.

The second observation concerns the structural properties of the labyrinth line graph. Channel graphs have frequently been used as secondary and topological descriptors of

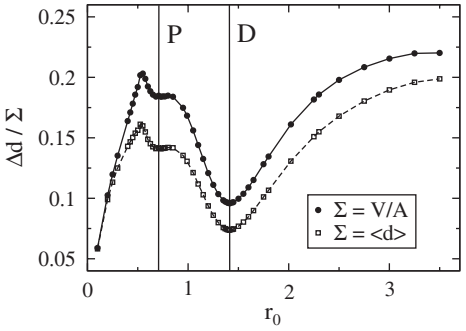

Fig. 3. Fluctuations of the distance function value d for the rPD family as a function of r_0.

IPMS [14–16]. As explained above, the MS can be readily reduced to a line graph. Applying that construction to the rPD reveals two somewhat interesting facts: (1) our definition of a geometrically centered line graph gives the expected change in connectivity (i.e., 4-connected for the D and 6-connected for the P surface) whereas a purely symmetry-based definition does not; (2) the geometrically centered line graph does contain edges that are not straight (see Fig. 2).

3. Conclusions and future work

We have shown that a MS analysis of extrinsic properties of the surface, rather than intrinsic curvature properties, is crucial to an understanding of the underlying graph structure of the transition from the P to the D surface.

We have also shown that fluctuations of a point-wise defined channel diameter are minimal for the member corresponding to the D surface, whereas they seem to be a horizontal inflection point at the P surface member.

The next step is a more comprehensive analysis of other IPMS families that will elucidate whether high-symmetry members of these families are always favored in terms of their homogeneity. The issue of an optimal transformation pathway between the P and D IPMS and, more generally, the P-Gyroid-D IPMS family, remains open. For example, deformations within the rhombohedral Gyroid (rG) family allow for a continuous transition path among IPMS, with all intermediates IPMS, from the (cubic) Gyroid via the D to the P surface. Explicit mathematical descriptions have been presented for two possible transformation routes, involving tetragonal and rhombohedral intermediates [17]. It is certain that lower symmetry routes also can be found, involving orthorhombic, monoclinic and indeed triclinic derivatives of the P and D families. The existence of these IPMS is assured [13], though detailed parametrizations have, to our knowledge, not been done. It is likely that lower symmetry paths are disfavored, given the decreasing curvature homogeneity with decreasing symmetry, though the possibility of comparably favorable tetragonal, rhombohedral and (for example) orthorhombic intermediates cannot be ruled dismissed a priori. These possibilities will be the focus

of our attention in the near future. In addition, the relative importance of intrinsic and extrinsic homogeneity measures to model relative stability of real material assemblies must be carefully assessed.

References

[1] L. Scriven, Equilibrium bicontinuous structure, Nature 263 (1976) 123–125.
[2] S. Hyde, S. Andersson, K. Larsson, Z. Blum, T. Landh, S. Lidin, B. Ninham, The Language of Shape, 1st Edition, Elsevier Science, Amsterdam, 1997.
[3] P. Barois, S. Hyde, B. Ninham, T. Dowling, Langmuir 6 (1990) 1136.
[4] K. Larsson, J. Phys. Chem. 93 (1989) 7304.
[5] M. Larsson, O. Terasaki, K. Larsson, A solid state transition in the tetragonal lipid bilayer structure at the lung alveolar surface, Solid State Sci. 5 (2003) 109–114.
[6] R. Templer, J. Seddon, N. Warrender, A. Syrykh, Z. Huang, R. Winter, J. Erbes, Inverse bicontinuous cubic phases in 2:1 fatty acid/phosphatidylcholine mixtures. The effects of chain length, hydration, and temperature, J. Phys. Chem. 102 (1998) 7251–7261.
[7] W. Helfrich, Z. Naturforsch. 28c (1973) 693.
[8] N. Medvedev, Dokl. Akad. Nauk. 337 (1994) 767.
[9] H. Blum, Biological shape and visual science (Part I), J. Theor. Biol. 38 (1973) 205–287.
[10] G. Schröder, S. Ramsden, A. Christy, S. Hyde, Medial surfaces of hyperbolic structures, Eur. Phys. J. B 35 (2003) 551–564.
[11] N. Amenta, S. Choi, R. Kolluri, The power crust, unions of balls, and the medial axis transform, Comput. Geom.: Theory Appl. 19 (2–3) (2001) 127–153.
[12] A. Fogden, S. Hyde, Parametrization of triply periodic minimal surfaces. I. Mathematical basis of the construction algorithm for the regular class, Acta Crystallogr. A 48 (1992) 442–451.
[13] A. Fogden, S. Hyde, Parametrization of triply periodic minimal surfaces. II. Regular class solutions, Acta Crystallogr. A 48 (1992) 575–591.
[14] W. Fischer, E. Koch, Genera of minimal balance surfaces, Acta Crystallogr. A 45 (1989) 726–732.
[15] A. Schoen, Infinite periodic minimal surfaces without self-intersections, Technical Report, NASA, 1970.
[16] S. Hyde, Curvature and the global structure of interfaces in surfactant–water systems, in: Colloque de Physique C7-1990, Supplément au Journal de Physique, 1990.
[17] A. Fogden, S. Hyde, Continuous transformations of cubic minimal surfaces, Eur. Phys. J. B 7 (1999) 91–104.